near touching) where the system can return to the ground state.[8,56]

A successful application of MNDOC to photochemical problems will thus require a reasonable description of these minima, barriers, and funnels. The presently available MNDOC results for excited states suggest the following preliminary assessment.

On the positive side, MNDOC treats $S_1$ and $T_1$ states with similar accuracy (see Tables I–III). Geometries of local minima are predicted reasonably well, both for "spectroscopic" and "biradicaloid" minima (see Table III). MNDOC is expected to provide a balanced description of different parts of the $S_1$ surface, including those parts where doubly excited configurations play an important role. For biradicaloid systems, MNDOC predicts the relative energies of covalent and zwitterionic states as well as the polarization in zwitterionic states in a qualitatively correct manner.

On the negative side, MNDOC energies and geometries are generally less accurate in excited states than in ground states. In particular, the excitation energies are systematically underestimated (cf. Tables I, II). This indicates that MNDOC will probably not predict funnels reliably especially in regions where the ground state is well represented by the closed-shell SCF configuration. Finally, no experience concerning MNDOC barriers in excited states is available yet.

On the basis of this evidence we believe that MNDOC can be applied in cautious explorations of excited-state surfaces. A more conclusive evaluation will only be possible after such applications have been carried out.

Future improvements of the MNDOC method should obviously attempt to correct for the systematic underestimation of excitation energies. For this purpose, excitation energies should be included as reference data in the parametrization procedure, rather than using ground-state data only. We have carried out some test calculations of this kind which suggest that better excitation energies can be obtained with modified MNDOC parameters but only at the expense of larger errors in the ground-state properties. An overall improvement of the MNDOC model would thus probably require the introduction of different parametric functions[11,15] rather than a mere variation of the MNDOC parameters.

## Conclusions

MNDOC is superior to MNDO for the treatment of excited states, although the errors in MNDOC energies and geometries are larger for excited states than for ground states. Excitation energies are systematically underestimated by MNDOC, whereas energy differences between excited states, geometries, and charge distributions in excited states are reproduced reasonably. The present evidence supports cautions applications of MNDOC to photochemical problems.

**Acknowledgment.** This work was supported by the Deutsche Forschungsgemeinschaft and the Fonds der Chemischen Industrie (through a Liebigstipendium). The calculations were carried out on the TR 440 computer of the Universität Marburg.

---

# Oxidation–Reduction Reactions of Complexes with Macrocyclic Ligands. Structure-Reactivity Relations and Reorganizational Barriers for Outer-Sphere Electron-Transfer Reactions of Low-Spin Cobalt(III)–Cobalt(II) Couples[1]

**John F. Endicott,* Bill Durham, Milton D. Glick, Thomas J. Anderson, James M. Kuszaj, William G. Schmonsees, and K. P. Balakrishnan**

*Contribution from the Department of Chemistry, Wayne State University, Detroit, Michigan 48202.* *Received May 15, 1980*

**Abstract:** A series of structurally homologous *trans*-Co($N_4$)($OH_2$)$_2^{3+,2+}$ couples has been developed and used to probe the intrinsic, $\Delta G_{i,ab}^\ddagger$, and thermodynamic, $\Delta G_{ab}^\circ$, components of electron-transfer reactivity. X-ray structural studies have been used to determine that only the axial Co–$OH_2$ bond lengths change across the electron-transfer reaction coordinate. The equatorial Co–N (macrocycle) bond lengths are independent of formal oxidation state but do depend on the type of nitrogen donor (amine or imine) of the 14-membered macrocyclic ligands. Variations of self-exchange electron-transfer rates in this series are found to be attributable to the reorganizational energies which result from changes in metal–ligand axial bond lengths. However, the observed activation barriers are consistently larger than predicted only on the basis of Franck–Condon and work terms. The nearly constant discrepancy in these $\sigma^*$–$\sigma^*$ exchanging systems, $\Delta G^\ddagger(\text{obsd}) - \Delta G^\ddagger(\text{calcd}) \simeq 10$ kJ mol$^{-1}$, is attributed to a small value for the electron-exchange term (in a quantum mechanical formulation) or the electronic transmission factor (in a semiclassical formulation). Intrinsic parameters, $\Delta G_{i,aa}^\ddagger$, are determined for several Co($N_4$)($OH_2$)$_2^{3+,2+}$ couples, and these parameters are used to isolate the $\Delta G_{ab}^\circ$ dependence of several cross reactions. It is found that $\Delta G_{ab}^\ddagger$ for cross reactions of these complexes depends on $\Delta G_{ab}^\circ$ very nearly as predicted in the classical models developed by Marcus.

## Introduction

The transfer of an electron between different complex ions with independent primary coordination spheres can occur at rates which span some 15–20 powers of ten.[2] On a molecular scale, these "outer-sphere" reactions approach a limit in which donor–acceptor interactions constitute an energetically insignificant perturbation

---

(1) (a) Partial support of this research by the National Institutes of Health (Grant AM 14341) is gratefully acknowledged. (b) Presented in part at the 172nd National Meeting of the American Chemical Society, San Francisco, Calif, Sept 1976, INOR 168.

(2) For recent reviews see: (a) Taube, H. "Electron Transfer Reactions of Complex Ions in Solution", Academic Press: New York, 1970; (b) Linck, R. G. *MTP Int. Rev. Sci.: Inorg. Chem., Ser. One* **1971**, *9*, 303; (c) *Int. Rev. Sci.: Inorg. Chem., Ser. Two* **1974**, *9*, 173; (d) *Surv. Prog. Chem.* **1976**, *7*, 89; (e) Sutin, N. In "Tunneling in Biological Systems"; Chance, B., DeVault, D. C., Frauenfelder, H., Marcus, R. A., Schreiffer, J. R., Sutin, N., Eds.; Academic Press: New York, 1979; p 201.

0002-7863/81/1503-1431$01.25/0

along the reaction coordinate. As a consequence, these reactions have received considerable theoretical attention.[4-11] When there is very little change of metal–ligand bond lengths across the reaction coordinate, the semiclassical theories of Marcus[4] and Hush[5] provide an excellent accounting for variations in reactivity.[2,12] However, when appreciable changes in metal–ligand bond length occur, deviations from the semiclassical models are often observed. Perhaps the most striking problems have been observed for reaction systems involving cobalt(III)–cobalt(II) ($d^6/d^7$) couples.[2] Illustrative of the peculiarities of the cobalt systems are the very large variations in self-exchange rates (i.e., in reactions with $\Delta G^\circ = 0$ as defined in eq 1) for closely related cobalt-

$$M^{III}L_6 + {}^*M^{II}L_6 \rightleftharpoons M^{II}L_6 + {}^*M^{III}L_6 \qquad (1)$$

(III)–cobalt(II) couples. Thus, for the $Co(NH_3)_6^{3+,2+}$, $Co(en)_3^{3+,2+}$, and $Co(sep)^{3+,2+}$ couples the self-exchange rate constants are reported to be $\leq 10^{-9}$,[13] $3.4 \times 10^{-5}$,[14,15] and 5 $M^{-1}\ s^{-1}$,[16,17] respectively. The source of this variation in rate constant is not immediately obvious since the ions differ only a little in size, all involve low-spin (singlet) cobalt(III) and high-spin (quartet) cobalt(II) and all appear to involve very similar changes in Co–N bond length across the reaction coordinate: 17 pm for $Co(sep)^{3+,2+}$[16] and 17.4 pm for $Co(NH_3)_6^{3+,2+}$.[18] Very recently the extraordinarily small self-exchange rate constant for the $Co(NH_3)_6^{3+,2+}$ couple has been ascribed[19] to a combination of a small transmission coefficient (arising from the spin-forbidden, weak coupling of donor and acceptor electronic wave functions) and small Franck–Condon overlap parameters (due to the large change in metal–ligand bond length). A feature of the electron-transfer models, which quantize the metal–ligand motions, is that the energy gap (or $\Delta G_{ab}^\circ$) is coupled to the terms which describe metal–ligand displacements across the reaction coordinate.[7,8,18] As a consequence a simple dependence of the rate constant (or $\Delta G_{ab}^*$) on the reaction driving force ($\Delta G_{ab}^\circ$) is not necessarily expected for reactions involving large changes in metal–ligand bond length.[8a,b,18] It is a further consequence of the quantum models that, as the critical vibrational quanta become large compared to $kT$, the "Franck–Condon" component of the activation barrier becomes nearly independent of temperature.[8,18]

Several years ago we commenced the study of electron-transfer reactions of cobalt(III)–cobalt(II) systems complexed by equatorial macrocyclic ligands.[19] Some of the early work indicated that the intrinsic barriers to electron transfer were large and of different magnitudes for different $Co(N_4)(OH_2)_2^{3+,2+}$ couples.[20] It seemed likely that origin of the intrinsic barriers in these systems was in large variations of cobalt–axial ligand bond lengths.[20d] X-ray structural work has confirmed that the low-spin $Co(N_4)(OH_2)_2^{2+}$ complexes are axially distorted and that there are indeed large differences in the axial $Co^{II}$–$OH_2$ bond lengths.[21]

This report describes our use of a series of structurally similar, low-spin, *trans*-$Co(N_4)(OH_2)_2^{3+,2+}$ couples to probe the reorganizational barriers in a variety of outer-sphere electron-transfer reactions. This study constitutes the first systematic investigation of the dependence of intrinsic electron-transfer reactivity on simple structural parameters of the reactants. We have also been able to investigate carefully the dependence of variations in electron-transfer rate on free-energy changes and on the intrinsic reactivities of the reaction partners for reactions involving large changes in metal–ligand bond length.

## Experimental Section

The synthesis and characterization of most of the complexes used in this study have been described elsewhere.[16,20-24] Other chemicals used were reagent grade.

*Warning*! The heavy metal perchlorates used in this study can be detonated and are potentially hazardous.

**Kinetic Techniques.** The cross reactions between macrocyclic complexes were slow and were run under pseudo-first-order conditions with $Co(N_4)(OH_2)_2^{3+}$ in excess. The reactions were monitored by means of the change in the absorbance of $Co(N_4)(OH_2)_2^{2+}$ using a Cary 14 spectrophotometer. The wavelengths monitored were (1) 540 nm for $Co(Me_4[14]tetraeneN_4)(OH_2)_2^{2+}$ ($\epsilon = 3250\ M^{-1}\ cm^{-1}$), (2) 570 nm for $Co(Me_2[14]1,11\text{-dieneN}_4\text{-13-one})(OH_2)_2^{2+}$ ($\epsilon = 760\ M^{-1}\ cm^{-1}$), and (3) 455 nm for $Co(Me_2pyo[14]trieneN_4)(OH_2)_2^{2+}$ ($\epsilon = 1261\ M^{-1}\ cm^{-1}$).

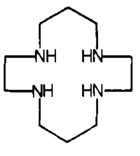

[14]aneN$_4$

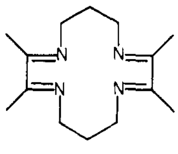

Me$_4$[14]tetraeneN$_4$

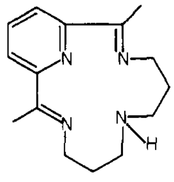

Me$_2$pyo[14]trieneN$_4$

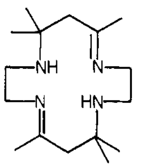

Me$_6$[14]4,11-dieneN$_4$

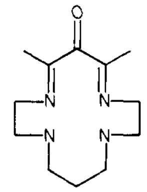

Me$_2$[14]1,11-dieneN$_4$-13-one

---

(3) Taube, H. *Can. J. Chem.* **1959**, *37*, 129.

(4) (a) Marcus, R. A. *Annu. Rev. Phys. Chem.* **1964**, *15*, 155. (b) *J. Phys. Chem.* **1963**, *67*, 853. (c) *Discuss. Faraday Soc.* **1960**, *29*, 21.

(5) (a) Hush, N. S. *Trans. Faraday Soc.* **1961**, *57*, 557. (b) *Prog. Inorg. Chem.* **1967**, *8*, 391. (c) *Electrochim. Acta* **1968**, *13*, 1005.

(6) (a) Efrima, S.; Bixon, M. *J. Chem. Phys.* **1976**, *64*, 3639. (b) *Chem. Phys.* **1976**, *13*, 447.

(7) (a) Van Duyne, R. P.; Fischer, S. F. *Chem. Phys.* **1974**, *5*, 183. (b) Fischer, S. F.; Van Duyne, R. P. *Ibid.* **1977**, *26*, 9.

(8) (a) Ulstrup, J.; Jortner, J. *J. Chem. Phys.* **1975**, *63*, 4358. (b) Kestner, N. R.; Logan, J. *J. Phys. Chem.* **1974**, *78*, 2148. (c) Jortner, J.; Ulstrup, J. *J. Am. Chem. Soc.* **1979**, *101*, 3744.

(9) Hoytink, G. J. In "Chemiluminescence and Bioluminescence"; Cormier, M. J., Hercules, D. M., Lee, J., Eds.; Plenum Press: New York, 1973; p 147.

(10) (a) Levich, V. G.; Dogonadze, R. R.; Kuznetsov, A. M. *Electrochim. Acta* **1968**, *13*, 1025. (b) Levich, V. G.; Dogonadze, R. R.; German, E. D.; Kuznetsov, A. M.; Kharkats, Yu. T. *Electrochim. Acta* **1970**, *15*, 353.

(11) (a) Brunschwig, B. S.; Logan, J.; Newton, M. D.; Sutin, N. *J. Am. Chem. Soc.* **1980**, *102*, 5798. (b) Newton, M. D. *Int. J. Quantum Chem., Quantum Chem. Symp.* **1980**, *No. 14*.

(12) Brown, G. M.; Sutin, N. *J. Am. Chem. Soc.* **1979**, *101*, 883.

(13) (a) Stranks, D. R. *Discuss. Faraday Soc.* **1960**, *29*, 73. (b) Birader, N. S.; Stranks, D. R. *Trans. Faraday Soc.* **1963**, *58*, 2421.

(14) Lewis, N. B.; Coryell, C. D.; Irvine, J. W. *J. Chem. Soc.* **1949**, 5386.

(15) Dwyer, F. P.; Sargeson, A. M. *J. Phys. Chem.* **1961**, *65*, 1892.

(16) (a) Creaser, I. I.; Harrowfield, J. Mac B.; Herit, A. J.; Sargeson, A. M.; Springborg, J.; Gene, R. J.; Snow, M. R. *J. Am. Chem. Soc.* **1977**, *99*, 3181. (b) Sargeson, A. M. *Chem. Br.* **1979**, *15*, 23.

(17) Abbreviations: Me$_4$[14]tetraeneN$_4$ = 2,3,9,10-tetramethyl-1,4,8,11-tetraazacyclotetradeca-1,3,8,10-tetraene; Me$_6$[14]4,11-dieneN$_4$ = 5,7,7,12,14,14-hexamethyl-1,4,8,11-tetraazacyclotetradeca-4,11-diene; [14]aneN$_4$ = 1,4,8,11-tetraazacyclotetradecane; Me$_2$pyo[14]trieneN$_4$ = 2,12-dimethyl-3,7,11,17-tetraazabicyclo[11.3.1]septadeca-1(17),2,11,13,15-pentaene; Me$_2$[14]1,11-dieneN$_4$-13-one = 12,14-dimethyl-1,4,8,11-tetraazacyclotetradeca-1,11-dien-13-one; sepulchrate = (*S*)-1,3,6,8,10,13,16,19-octaazabicyclo[6.6.6]eicosane.

(18) Stynes, H. C.; Ibers, J. A. *Inorg. Chem.* **1971**, *10*, 2304.

(19) Buhks, E.; Bixon, M.; Jortner, J.; Navon, G. *Inorg. Chem.* **1979**, *18*, 2014.

(20) (a) Liteplo, M. P.; Endicott, J. F. *Inorg. Chem.* **1971**, *10*, 1420. (b) Rillema, D. P.; Endicott, J. F.; Patel, R. C. *J. Am. Chem. Soc.* **1972**, *94*, 394. (c) Rillema, D. P. Endicott, J. F. *Inorg. Chem.* **1972**, *11*, 2361. (d) *J. Am. Chem. Soc.* **1972**, *94*, 8711. (e) Rillema, D. P.; Endicott, J. F.; Kane-Maguire, N. A. P. *Chem. Commun.* **1972**, 495. (f) Rillema, D. P.; Endicott, J. F. *Inorg. Chem.* **1976**, *15*, 1459.

(21) (a) Glick, M. D.; Kuszaj, J. M.; Endicott, J. F. *J. Am. Chem. Soc.* **1973**, *95*, 5097. (b) Glick, M. D.; Schmonsees, W. G.; Endicott, J. F. *Ibid.* **1974**, *96*, 5661. (c) Endicott, J. F.; Lilie, J.; Kuszaj, J. M.; Ramaswamy, B. S.; Schmonsees, W. G.; Simic, M. G.; Glick, M. D.; Rillema, D. P. *Ibid.* **1977**, *99*, 429. (d) Durham, B.; Anderson, T. J.; Switzer, J. A.; Endicott, J. F.; Glick, M. D. *Inorg. Chem.* **1977**, *16*, 271.

(22) (a) Rillema, D. P.; Endicott, J. F.; Barber, J. *J. Am. Chem. Soc.* **1973**, *95*, 6987. (b) Wong, C. L.; Switzer, J. A.; Balakrishnan, K. P.; Endicott, J. F. *Ibid.* **1980**, *102*, 5511.

(23) (a) Jackels, S. C.; Farmery, K.; Barefield, E. K.; Rose, N.; Busch, D. H. *Inorg. Chem.* **1972**, *11*, 2893. (b) Long, K. M.; Busch, D. H. *J. Coord. Chem.* **1974**, *4*, 113.

(24) (a) Barraclough, C. G.; Lawrence, G. A. *Inorg. Nucl. Chem. Lett.* **1976**, *12*, 133. (b) Hay, R. W.; Jeragh, B. *J. Chem. Soc., Dalton Trans.* **1977**, 1261.

For reactions with half-lives shorter than about 4 h, reactant solutions were deaerated separately by using $Cr^{2+}$-scrubbed Ar, and standard syringe techniques (Teflon or Pt needles) were used to mix reactant solutions in 1-cm, serum capped cuvettes. Mixing times were on the order of 10 s. For reactions with longer half-lives we fabricated an all-glass apparatus which permitted us to degas reactant solutions by using freeze–thaw cycles and then mix and transfer the reactant solutions to a cuvette fused to the same apparatus. All reactant solutions were thermostated at 25.0 ± 0.1 °C, except when otherwise indicated.

Reactant solutions of $Co([14]aneN_4)(OH_2)_2^{2+}$ were prepared very shortly before use by mixing deaerated solutions of the free ligand with deaerated solutions of $Co^{2+}$. Very similar procedures are described elsewhere.[22b,25]

Kinetic data for most of these reactions fit the pseudo-first order treatment for more than three reaction half-lives.

Reactions of $Ru(bpy)_3^{2+}$ were studied employing flash photolysis techniques similar to those described elsewhere.[26] Ruthenium(III) complexes were generated in the flash pulse by either of two techniques: (a) reactions 2–4 or (b) reactions 2 and 5 followed by (4). Approach b

$$Ru^{II}(bpy)_3 + h\nu \rightarrow {}^*Ru(bpy)_3 \tag{2}$$

$$^*Ru(bpy)_3 + M^{III}(N_4)XY \rightarrow Ru^{III}(bpy)_3 + M^{II}(N_4)XY \tag{3}$$

$$Ru^{III}(bpy)_3 + M^{II}(N_4)XY \rightarrow Ru^{II}(bpy)_3 + M^{III}(N_4)XY \tag{4}$$

was preferred since it allowed us to run reactions under pseudo-first-order conditions.

$$^*Ru(bpy)_3 + Co(NH_3)_5OH_2{}^{3+} \xrightarrow{H^+} Ru^{III}(bpy)_3 + Co^{2+} + 5NH_4{}^+ \tag{5}$$

**X-ray Techniques and Procedures.**[27] **$[Co(Me_6[14]4,11\text{-}dieneN_4)(NH_3)_2](ClO_4)_3$. Structural Analysis.** A crystal of dimensions 0.12 × 0.43 × 0.31 × 0.29 mm was mounted with Silastic adhesive on a glass fiber. Precession photographs (Cu K$\alpha$) gave preliminary lattice constants and showed absences consistent with the monoclinic space groups *Aa* or *A*2/*a*. A piezoelectric test showed no resonances, so *A*2/*a* was assigned as the probable space group. The crystal was then mounted on a card-controlled Picker diffractometer equipped with Mo K$\alpha$ radiation for the remaining studies. Least-squares analysis of 35 reflections centered with Mo K$\alpha_1$ radiation ($\lambda$ = 70.926 pm) yielded the following unit-cell information: $a$ = 959.6 (0.9) pm, $b$ = 1882.9 (1.6) pm, $c$ = 1555.0 (1.4) pm, $\beta$ = 86.09 (2)°, $V$ = 2.803 nm$^3$, $\rho$(flotation) = 1.59 (1) g/mL, $\rho$(calcd) = 1.59 g/mL, $Z$ = 4, $\mu$ = 10.0 cm$^{-1}$.

Intensity data were collected by the $\theta$–$2\theta$ scan method with Zr-filtered Mo K$\alpha$ radiation. A symmetric scan of 2.0° plus an allowance for spectral dispersion was used with a scan rate of 2.0°/min. Stationary background counts of 15 s were taken at each end of the scan. Four standard reflections varied less than 5% throughout data collection. Standard deviations were assigned in accord with those of Radonovich and Glick[28] with an instability factor of 0.05. No absorption corrections were made. Of the 2571 data examined with $2\theta \le 50$, 1533 data with $I > 2.5\sigma(I)$ were used throughout the solution and refinement of the structure.

Examination of the three-dimensional Patterson synthesis yielded the position of the cobalt ion on the inversion center at $0,{}^1/_4,{}^1/_4$. Subsequent three-dimensional Fourier maps allowed the unambiguous positioning of all nonhydrogen atoms except one perchlorate ion, which appeared to be disordered about the twofold axis at ${}^1/_4a$, 0$c$. Full-matrix isotropic least-squares refinement at this point resulted in discrepancy factors of $R = \sum||F_o| - |F_c||/\sum|F_o|$ = 0.219 and $R_w = [w(|F_o| - |F_c|)^2/w|F_o|^2]^{1/2}$ = 0.310. A difference synthesis revealed the disorder involved two tetrahedral perchlorate groups related by the twofold axis with the chlorine atoms separated by 0.802 Å. Two cycles of full-matrix anisotropic refinement on the disordered model resulted in $R$ = 0.077 and $R_w$ = 0.096. A Fourier difference synthesis revealed the positions of all hydrogen atoms. A cycle of anisotropic least-squares refinement, with fixed contributions from the hydrogen atoms, produced final discrepancy factors of $R$ = 0.066 and $R_w$ = 0.082, an error of fit of 2.26 and a maximum residual electron density of 400 e/nm$^3$. An attempt to refine the structure in the acentric space group *Aa* gave no significant improvement in discrepancy factors and chemically less satisfying bond distances and angles.

**$[Co(Me_4[14]tetraeneN_4)(NH_3)_2]Br_3\cdot 2H_2O$. Structural Analysis.** A single crystal of approximate dimensions 0.20 × 0.25 × 0.22 mm was mounted with Silastic adhesive on a glass fiber. Weissenberg photographs (Mo K$\alpha$) gave preliminary lattice constants and showed absences consistent with the monoclinic space group $P2_1/c$. The remaining studies were carried out on a Syntex P2$_1$ diffractometer with Nb-filtered Mo K$\alpha$ radiation. Least-squares analysis of 15 reflections with $2\theta > 25°$ centered with Mo K$\bar{\alpha}$ radiation ($\lambda$ = 71.069 pm) yielded the following unit-cell information: $a$ = 1782.9 (3) pm, $b$ = 965.6 (1) pm, $c$ = 1822.0 (3) pm, $\beta$ = 133.11 (1)°, $V$ = 229.0 nm, $\rho$(flotation) = 1.75 (2) g/mL, $\rho$(calcd) = 1.789 g/mL, $Z$ = 4, $\mu$ = 65.8 cm$^{-1}$.

Intensity data were collected by the $\theta$–$2\theta$ scan technique with a scan range from K$\alpha_1$ − 0.75° to K$\alpha_2$ + 0.90° and background counts at each end of the scan equal to half the total scan time. The scan rate varied inversely with the peak intensity from 1°/min to 29°/min. Three standard reflections, examined every 100 data, showed a gradual decrease in intensity totalling 12%, which was corrected for. No absorption corrections were made. Standard deviations were assigned with an instability factor of 0.05. Of the 3241 data examined, the 1599 data for which $I > \sigma(I)$ were used throughout the solution and refinement process.

An iterative application of the $\Sigma_2$ relationship[29] was used on 270 normalized structure factors of magnitude 1.3 or greater. An $E$ map based upon the best solution ($C$ = 0.88, 3 cycles) yielded a model in which the Co atoms are located on inversion centers and the Br atoms are in general positions. Fourier difference maps then were used to locate the two independent halves of macrocycles. Isotropic least-squares refinement yielded $R$ = 0.183. Inclusion of two peaks from the difference maps (5 × 10$^3$ e/nm$^3$) as waters of crystallization reduced $R$ to 0.157. Inclusion of anomalous dispersion corrections and the use of anisotropic thermal parameters for Co and Br resulted in $R$ = 0.085. Anisotropic refinement on all atoms yielded $R$ = 0.076 and $R_w$ = 0.097 and an error of fit of 3.12.

In order to obtain a better weighting scheme, following Hoard,[30] we calculated standard deviations according to $\sigma(F) = \sum a_n|F_o|n$.[3] Moreover, the tendency of Nb filters to yield low-angle data for which $F_o > F_c$, due to poor background estimates, has been noted by Ibers.[31] The 67 data for which $2\theta < 13°$ did show this trait and also had anomalous background distribution and were eliminated. Final full-matrix anisotropic least-squares refinement with the revised weighting scheme converged with $R$ = 0.067 and $R_w$ = 0.086 and an error of fit of 1.05. The maximum residual electron density of 800 e/nm$^3$ was near the Br atoms.

**$[Fe(Me_4[14]tetraeneN_4)(OH_2)_2](ClO_4)_3\cdot H_2O$. Structural Analysis.** The three-dimensional single-crystal structure determination was conducted on crystals obtained by recrystallization of the compound from 1 M $HClO_4$. A suitable orange-red crystal of dimensions 0.19 × 0.23 × 0.33 mm was glued onto a glass fiber with epoxy cement.

Rotation and axial photographs of the crystal on a Syntex P2$_1$ diffractometer, together with a small set of intensity data, were consistent with Laue symmetry $P\bar{1}$. A cell reduction[32] failed to find a cell of higher symmetry. Fifteen reflections with $2\theta$ (Mo K$\bar{\alpha}$, $\lambda$ = 71.069 pm) between 15 and 25° were centered automatically. The cell parameters are $a$ = 1241.6 (3) pm, $b$ = 1270.6 (3) pm, $c$ = 894.0 (0.2) pm, $\alpha$ = 92.59 (2)°, $\beta$ = 104.62 (2)°, $\gamma$ = 89.70 (2)°, $V$ = 1.363 nm$^3$, $\rho$(flotation) = 1.60 (2) g/mL, $\rho$(calcd) = 1.599 g/mL, $Z$ = 2, $\mu$ = 9.18 cm$^{-1}$.

Intensity data were collected by using Mo K$\alpha$ radiation which had been diffracted from a highly oriented graphite crystal in the parallel geometry. The $\theta$–$2\theta$ scan technique was used with a scan rate of 2.02°/min. The backgrounds were estimated at each end of the scan by counting for a total of half the time of the scan. During data collection, the intensities of three standard reflections were measured every 97 reflections, with no indication of decomposition. No absorption correction was made. Standard deviations were assigned with an instability factor of 0.05. Of 3979 data examined ($2\theta_{Mo} < 45°$), the data for which $I > 2.5\sigma(I)$ were used throughout the solution and refinement process.

---

(25) Endicott, J. F.; Balakrishnan, K. P.; Wong, C. L. *J. Am. Chem. Soc.* **1980**, *102*, 5519.

(26) (a) Ferraudi, G. J.; Endicott, J. F. *Inorg. Chem.* **1973**, *12*, 2389. (b) *Ibid.* **1977**, *16*, 2762. (c) *Inorg. Chim. Acta* **1979**, *37*, 219.

(27) Local versions of the following major programs were used in the solution and refinement of structures in this work: (a) SYNCOR, W. Schmonsees' program for data reduction; (b) DACOR, D. L.Smith's program for data reduction; (c) FORDAP, A. Zalkins' Fourier program; (d) ORFLS and ORFEE, W. R. Busing, K. O. Martin, and H. A. Levy's full-matrix least-squares program and function and error program; (e) ORTEP, C. K. Johnson's program for drawing crystal models. Scattering factors including the anomalous scattering terms were taken from "International Tables for X-ray Crystallography"; Ibers, J. A., Hamilton, W., Eds.; Kynoch Press: Birmingham, England, 1974; Vol. IV. The program HFINDR (A. Zalkin) was used to assign hydrogen positions from carbon atoms with idealized angles.

(28) Radonovich, L.; Glick, M. D. *Inorg. Chem.* **1978**, *10*, 1463.

(29) Long, R. E. Ph. D. Thesis (Part III), University of California, Los Angeles, Calif., 1965.

(30) Collins, D. M.; Hoard, J. L. *J. Am. Chem. Soc.* **1970**, *92*, 3761.

(31) Manajlovic-Muir, L.; Muri, K. W.; Ibers, J. A. *Inorg. Chem.* **1970**, *9*, 447.

(32) TRACER, S. Lawton and R. A. Jacobson's program for cell reduction.

Table I. Important Distances (pm) and Angles (Deg)[a]

| | $[Co(Me_6[14]$-4,11-diene$N_4)$-$(NH_3)_2](ClO_4)_3$ | $[Co(Me_4[14]$tetraene$N_4)$-$(NH_3)_2]Br_3\cdot 2H_2O$ | | $[Co(Me_4[14]$tetraene$N_4)$-$(OH_2)_2](ClO_4)_3\cdot H_2O$ | | $[Fe(Me_4[14]$tetraene$N_4)$-$(OH_2)_2](ClO_4)_3\cdot H_2O$ | |
|---|---|---|---|---|---|---|---|
| | | 1 | 2 | 1 | 2 | 1 | 2 |
| Nd–C1–C2 | 106.3 (7) | 111 (1) | 112 (1) | 111.6 (4) | 112.2 (5) | 112.4 (5) | 112.1 (5) |
| C1–C2–C3 | 118.6 (5) | 118 (1) | 113 (1) | 114.9 (6) | 114.8 (6) | 116.0 (6) | 115.4 (6) |
| C2–C3–N2 | 121.4 (8) | 113 (1) | 113 (1) | 112.6 (5) | 112.5 (5) | 112.9 (5) | 112.5 (5) |
| C3–N2–C4 | 119.4 (7) | | | 121.6 (5) | 122.4 (5) | 122.5 (5) | 122.3 (5) |
| N2–C4–C5 | 107.5 (6) | 113 (1) | 113 (1) | 114.3 (5) | 113.1 (5) | 113.9 (5) | 113.2 (5) |
| C4–C5–N1′ | 105.3 (7) | 113 (1) | 114 (1) | 113.1 (5) | 114.4 (5) | 113.5 (5) | 114.1 (5) |
| C5–N1′–C1′ | 115.5 (6) | | | 120.6 (5) | 120.8 (5) | 122.2 (5) | 121.2 (5) |
| M–N1–C1 | 121.2 (5) | 124 (1) | 122 (1) | 123.5 (4) | 123.9 (4) | 121.7 (4) | 123.1 (4) |
| M–N1–C5′ | 107.3 (5) | 113 (1) | 116 (1) | 115.4 (4) | 115.1 (4) | 115.7 (4) | 115.4 (4) |
| M–N2–C3 | 129.2 (6) | 123 (1) | 125 (1) | 123.4 (4) | 122.2 (4) | 121.2 (4) | 121.6 (4) |
| M–N2–C4 | 111.4 (5) | 116 (1) | 115 (1) | 114.8 (4) | 115.1 (4) | 116.2 (4) | 116.9 (4) |
| N1–M–N2 | 94.2 (3) | 99 (1) | 99 (1) | 98.0 (2) | 98.0 (2) | 99.5 (2) | 99.1 (2) |
| N1–M–N2′ | 85.8 (3) | 81 (1) | 81 (1) | 82.0 (2) | 82.0 (2) | 80.5 (2) | 80.9 (2) |
| N1–M–X | 93.0 (3) | 93 (1) | 91 (1) | 93.1 (2) | 92.1 (2) | 92.8 (2) | 92.6 (2) |
| N1–M–X′ | 87.0 (3) | 87 (1) | 89 (1) | 86.9 (2) | 87.9 (2) | 87.2 (2) | 87.4 (2) |
| N2–M–X | 91.6 (3) | 89 (1) | 91 (1) | 92.4 (2) | 92.9 (2) | 91.3 (2) | 91.2 (2) |
| N2–M–X′ | 88.4 (3) | 91 (1) | 89 (1) | 87.6 (2) | 87.1 (2) | 88.7 (2) | 88.8 (2) |
| N1–C1 | 152 (1) | 148 (2) | 147 (2) | 146.4 (0.8) | 147.7 (7) | 146.6 (8) | 147.0 (7) |
| C1–C2 | 152 (1) | 152 (2) | 155 (3) | 151.0 (0.9) | 150 (1) | 151 (1) | 152 (1) |
| C2–C3 | 1.50 (1) | 1.52 (2) | 1.55 (2) | 149.3 (0.9) | 149 (1) | 148 (1) | 151 (1) |
| C3=N2 | 128 (1) | 150 (2) | 146 (2) | 146.9 (0.8) | 146.1 (0.8) | 148.4 (0.8) | 147.0 (0.8) |
| N2–C4 | 148 (1) | 127 (2) | 126 (2) | 127.9 (0.8) | 128.1 (0.7) | 126.6 (0.8) | 128.0 (7) |
| C4–C5 | 154 (1) | 147 (2) | 149 (3) | 150.0 (0.9) | 150.7 (0.9) | 150.2 (0.9) | 150.4 (0.9) |
| C5–N1′ | 147 (1) | 129 (2) | 128 (2) | 127.9 (0.7) | 126.0 (8) | 127.3 (0.7) | 127.3 (0.7) |
| C4–C4M | | 150 (3) | 152 (3) | 150.0 (0.9) | 157.9 (0.9) | 150.6 (0.9) | 147.3 (9) |
| C5–C5M | | 152 (2) | 154 (3) | 148.3 (0.8) | 150.2 (0.8) | 149.4 (0.8) | 149.7 (0.8) |
| C1–C1M1 | 152 (1) | | | | | | |
| C1–C1M1 | 155 (1) | | | | | | |
| C3–C3M | 154 (1) | | | | | | |
| Co–N1 | 198.6 (0.6) | 192 (1) | 193 (1) | 193.1 (4) | 193.2 (0.5) | | |
| Fe–N1 | | | | | | 195.9 (0.5) | 195.4 (0.4) |
| Co–N2 | 191.6 (0.7) | 190 (1) | 193 (1) | 192.8 (0.4) | 193.1 (0.4) | | |
| Fe–N2 | | | | | | 194.8 (0.5) | 194.7 (0.5) |
| Co–Xw | | | | 191.3 (0.4) | 191.3 (0.4) | | |
| Fe–Xw | | | | | | 190.1 (0.4) | 191.2 (0.4) |
| CoXamm | 195.4 (0.6) | 197 (1) | 197 (1) | | | | |
| FeXamm | | | | | | | |

[a] The primed atoms are related to the unprimed atoms by the inversion center at the appropriate metal atom. The headings 1 and 2 correspond to the symmetry-independent half-molecules present in three of the four crystals. The estimated standard deviations of the last digit(s) are given in parentheses.

The structure was solved by Patterson and Fourier techniques in the centric space group $P\bar{1}$. The iron(III) ions were located at the center of inversion at (0,0,0) and $(^1/_2,^1/_2,^1/_2)$. Full-matrix least-squares refinement of all nonhydrogen coordinates and isotropic thermal parameters refined to discrepancy factors of $R = 0.093$ and $R_w = 0.102^3$. Because of the large number of variables, refinement was continued by the block-diagonal approximation. Block-diagonal least-squares refinement of nonhydrogen coordinates and anisotropic thermal parameters converged to $R = 0.055$ and $R_w = 0.077$ and an error of fit of 1.02. During refinement the contribution of hydrogen atoms was included by assigning positions corresponding to C–H and O–H bond distances of 97 pm in expected geometries and by using isotropic thermal parameters 10% greater than the isotropic equivalent of the atom to which the hydrogen is bonded. A final difference Fourier map showed no residual peaks greater than 300 e/nm$^3$.

**$[Co(Me_4[14]$tetraene$N_4)(OH_2)_2](ClO_4)_3\cdot H_2O$.** The X-ray experimental procedure just described for the Fe complex was followed for the corresponding Co complex. A crystal of dimensions 0.17 × 0.25 × 0.31 mm was used for the study. The unit cell parameters are $a = 1234.2$ (0.4) pm, $b = 1265.5$ (0.4) pm, $c = 898.5$ (0.2) pm, $\alpha = 92.61$ (2)°, $\beta = 105.34$ (2)°, $\gamma = 89.91$ (2)°, $V = 1.352$ nm$^3$, $\rho$(flotation) = 1.61 (2) g/mL, $\rho$(calcd) = 1.621 g/mL, $Z = 2$, $\mu = 10.02$ cm$^{-1}$. Of the 3755 data examined ($2\theta$, Mo K$\alpha$ < 45°), 2868 were used during the solution and refinement process. The Co and Fe complexes were found to be isomorphous. Block-diagonal anisotropic least-squares refinement (with fixed hydrogen atom contributions as described above) converged to $R = 0.052$, $R_w = 0.066$, an error of fit of 1.00, and a residual electron density less than 270 e/nm$^3$.

## Results

**A. Description of Structures.** The labeling used for the three crystallographically different structures is given in Figure 1.

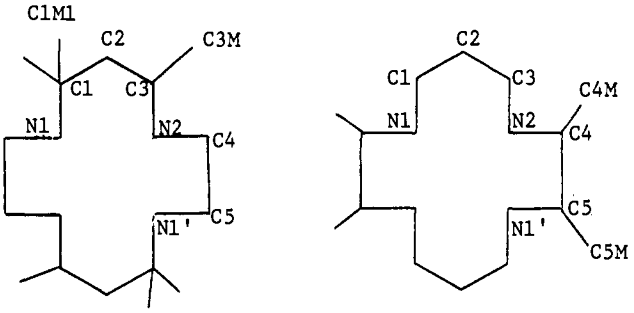

$Me_6[14]4,11$-diene$N_4$ $Me_4[14]$tetraene$N_4$

**Figure 1.** Labeling of structures and atoms.

Atomic parameters are listed in Tables S1–S4.[33]

All four of the complexes studied are comprised of a low-spin metal(III) ion coordinated to four nitrogenous donor sites of the macrocycle and to two axial ligands. The metal(III) ion in all cases is on a crystallographic center of inversion; thus, all compounds have crystallographic molecular symmetry $\bar{1}$ with the metal(III) ion centered in the equatorial plane. All bonds to the metal centers fall in the range of 191–197 pm.

The equatorial bond lengths for the cobalt(III) complexes are almost the same as those we have found for the corresponding

---

[33] See paragraph at end of paper for supplementary material.

Table II. Coordination Sphere Bond Lengths of Some Macrocyclic Complexes[a]

| complex | equatorial M–N imine | equatorial M–N amine | axial M–X |
|---|---|---|---|
| $Co(Me_4[14]tetraeneN_4)(OH_2)_2^{3+}$ | 191 | | 191 |
| $Co(Me_4[14]tetraeneN_4)(NH_3)_2^{3+}$ | 193 | | 197 |
| $Co(Me_6[14]4,11\text{-}dieneN_4)(NH_3)_2^{3+}$ | 192 | 199 | 195 |
| $Co(Me_4[14]tetraeneN_4)Cl_2^{+}$ | 192[b] | | 224[b] |
| $Co(Me_2[14]1,11\text{-}dieneN_4\text{-}13\text{-}one)Cl_2^{+}$ | 192[c] | 198[c] | 224[c] |
| $Co(Me_4[14]tetraeneN_4)(OH_2)_2^{2+}$ | 190[d] | | 229[d] |
| $Co(Me_2[14]1,11\text{-}dieneN_4\text{-}13\text{-}one)(OH_2)_2^{2+}$ | 192[c] | 198[c] | 228, 239[c] |
| $Co(Me_6[14]4,11\text{-}dieneN_4)(OH_2)_2^{2+}$ | 192[d] | 198[d] | 248[d] |
| $Fe(Me_4[14]tetraeneN_4)(OH_2)_2^{3+}$ | 195 | | 191 |
| $Fe(Me_4[14]tetraeneN_4)(NCCH_3)_2^{2+}$ | 195[e] | | 191[e] |
| $Ni(Me_4[14]tetraeneN_4)(imidazolate)_2$ | 201[f] | | 216[f] |

[a] This work except as indicated. All the cobalt and iron complexes are low spin. Bond lengths in pm and rounded off to the nearest pm. [b] Reference 34c. [c] Reference 21d. [d] Reference 21c. [e] Reference 34a. [f] Reference 34b. High-spin nickel(II).

$Co^{II}(N_4)(OH_2)_2$ complexes.[21c] The Fe–N bonds in $Fe(Me_4[14]tetraeneN_4)(OH_2)_2^{3+}$ are longer than the equatorial bond lengths in $Co(Me_4[14]tetraeneN_4)(OH_2)_2^{3+}$ or in $Co(Me_4[14]tetraeneN_4)(OH_2)_2^{2+}$ (see Table II). This does not result in any significant difference in the torsion angles of the six-membered chelate rings. It is interesting that the axial bond lengths in these complexes are essentially equal to one another and approximately the same as the equatorial Co–N bond lengths. The equatorial expansion in the iron(III) complex constitutes an uncommon tetragonal distortion. A small effect on the molecular geometry is not unexpected for a Jahn–Teller distortion in a low-spin $d^5$ complex.

The large variation in axial low-spin cobalt(II)–ligand bond lengths has been previously discussed.[21c] In the cobalt(III) structures, axial bond lengths vary with the nature of the axial donor atom but not with variations in the equatorial ligand (Table II).

**B. Kinetic Studies.** We have investigated several reactions of the type

$$Co(N_4)(OH_2)_2^{3+} + Co(N_4')(OH_2)_2^{2+} \underset{k_{ba}}{\overset{k_{ab}}{\rightleftharpoons}} Co(N_4)(OH_2)_2^{2+} + Co(N_4')(OH_2)_2^{3+} \quad (6)$$

with the cobalt(III) complex as excess reagent. These experiments are summarized in Table III. The diaquocobalt(III) complexes are all quite acidic ($pK_a \approx 3$–$4$). Since electron transfer in the $Co^{III,II}(N_4)$ couples is particularly favored in inner-sphere pathways, one would anticipate some problems due to hydroxy-bridged pathways. As a consequence most of our studies have been performed in 1 M $HClO_4$. We have examined several of the systems for the expected pH-dependent electron-transfer rates. We have used $Co([14]aneN_4)(OH_2)_2^{2+}$ as the reductant in these studies for reasons of convenience and since we expected the maximum pH effects with this reductant: (1) this is one of the stronger reducing agents we have used; (2) $Co([14]aneN_4)(OH_2)_2^{3+}$ is sufficiently acidic that free-energy changes should not greatly complicate the observations; (3) stereochemical constraints should be minimal with this complex. However, it should be noted that the stereochemistry of the macrocycle complexes is expected to favor linear bridging, and this should reduce the importance of the hydroxy bridge. Data in Table III indicate that the hydroxy-bridged pathway is not important in these systems in strongly acidic solutions.

We have also determined the rate constants for several cross reactions involving only one macrycyclic complex reactant. These studies are summarized in Table IV, and the results of these studies are presented in Figures 2, 5, and 6 below.

## Discussion

**A. Structural Variations in the Macrocyclic Complexes.** The data collected in Table II indicate that the equatorial Co–N(imine) and Co–N(amine) bond lengths are constant (192 ± 1 and 198 ± 1 pm, respectively) for complexes with 14-membered macrocyclic ligands. It is especially surprising that the variations in formal oxidation state should have so little effect on the equatorial,

Table III. Rate Constants for $Co(N_4)(OH_2)_2^{3+}$ and $Co(N_4')(OH_2)_2^{2+}$ Reactions

| $N_4$ | $N_4'$ | $\Delta E^f$,[a] V | $k$,[b] $M^{-1}\,s^{-1}$ |
|---|---|---|---|
| $Me_2pyo[14]trieneN_4$ | $Me_4[14]tetraeneN_4$ | 0.003 | 0.07 ± 0.01 (5) |
| | $[14]aneN_4$ | 0.146 | 0.085 |
| | $[14]aneN_4$ | 0.146 | 0.063[c] |
| $Me_4[14]tetraeneN_4$ | $[14]aneN_4$ | 0.143 | 0.11 ± 0.01 (2) |
| | $[14]aneN_4$ | 0.143 | 0.16 ± 0.03 (2)[c] |
| | $[14]aneN_4$ | 0.143 | 0.13 ± 0.01 (3)[d] |
| $Me_2[14]1,11\text{-}dieneN_4\text{-}13\text{-}one$ | $Me_2pyo[14]trieneN_4$ | 0.033 | 0.046 ± 0.001 (3) |
| | $Me_4[14]tetraeneN_4$ | 0.036 | 0.025 ± 0.006 (5)[e] |
| | $[14]aneN_4$ | 0.179 | 0.18 |
| | $[14]aneN_4$ | 0.179 | 0.10 ± 0.01 (2)[c] |
| | $[14]aneN_4$ | 0.179 | 0.25[f] |
| | $[14]aneN_4$ | 0.179 | 0.31[g] |
| $Me_6[14]4,11\text{-}dieneN_4$ | $Me_2pyo[14]trieneN_4$ | −0.003 | $(2.0 \pm 0.3) \times 10^{-3}$ (3) |
| | $Me_4[14]tetraeneN_4$ | 0.000 | $(1.3 \pm 0.1) \times 10^{-3}$ (2) |

[a] Based on formal potentials determined at 25 °C, $\mu = 0.10$ ($HClO_4$): (i) Yee, E. L.; Cave, R. J.; Guyer, K. L.; Tyma, P. D.; Weaver, M. J. *J. Am. Chem. Soc.* 1979, *101*, 1131. (ii) Yee, E. L.; Weaver, M. J., private communication from M.J.W., 1979. [b] 25 °C, 1.0 M $HClO_4$. [c] 25 °C, 0.5 M $HClO_4$. [d] 25 °C, 0.9 M $LiClO_4$, 0.1 M $HClO_4$. [e] Based on data at 35.5, 30.5, 29.5, 25, and 20 °C, $\Delta H^{\ddagger} = 42 \pm 8$ kJ $mol^{-1}$ and $\Delta S^{\ddagger} = -105 \pm 12$ J $mol^{-1}\,deg^{-1}$. [f] 25 °C, 0.5 M $HClO_4$, 0.5 M $LiClO_4$. [g] 25 °C, 0.5 M $HClO_4$, 0.5 M $NaClO_4$.

Table IV. Self-Exchange and Thermodynamic Parameters for $Co(N_4)(OH_2)_2^{3+,2+}$ Couples

| $N_4$ | $E^f$,[a] V | $S_{rc}$,[a] kJ $mol^{-1}\,deg^{-1}$ | $\Delta G_{aa}^{\ddagger}$,[b] kJ $mol^{-1}$ | $k_{aa}$,[c] $M^{-1}\,s^{-1}$ |
|---|---|---|---|---|
| $Me_4pyo[14]trieneN_4$ | 0.567 | 121 | 69.4 ± 0.8 | 0.093 ± 0.03 (3) |
| $Me_4[14]tetraeneN_4$ | 0.564 | 105 | 71.1 ± 0.8 | 0.050 ± 0.020 (3) |
| $Me_2[14]1,11\text{-}dieneN_4\text{-}13\text{-}one$ | 0.600 | 138 | 77.4 ± 1.6 | $(4.4 \pm 0.5) \times 10^{-3}$ (1) |
| $[14]aneN_4$ | 0.421 | 150 | 81.2 ± 0.8 | $(8 \pm 3) \times 10^{-4}$ (2) |
| $Me_6[14]4,11\text{-}dieneN_4$ | 0.564 | 188 | 88.7 ± 1.2 | $(4.5 \pm 2.0) \times 10^{-5}$ (1) |

[a] See note *a* of Table III. Potentials vs. NHE. [b] Best fit values for reactions in Table III; based on eq 7. 25 °C, 1.0 M $HClO_4$. [c] Same as note *b*. Numbers in parentheses are the number of different couples used for each determination.

Table V. Force Constants and Frequencies Inferred from Figure 3

| complex | $r_{II}$, pm | $r_{III}$, pm | $f_{II}$, N m$^{-1}$ | $f_{III}$, N m$^{-1}$ | $\omega_{II}$, cm$^{-1}$ | $\omega_{III}$, cm$^{-1}$ |
|---|---|---|---|---|---|---|
| $Co(Me_4[14]tetraeneN_4)(OH_2)_2$ | 229 | 191 | 56 | 196 | 260 | 434 |
| $Co(Me_2[14]1,11\text{-}dieneN_4\text{-}13\text{-}one)(OH_2)_2$ | 234 | 191 | 52 | 196 | 251 | 434 |
| $Co(Me_6[14]4,11\text{-}dieneN_4)(OH_2)_2$ | 248 | 191 | 39 | 196 | 217 | 434 |
| Co(sep) | 216 | 199 | 75 | 171 | 301 | 413 |

[a] Subscripts II and III refer to the formal oxidation states of the cobalt center.

Co–$N_{eq}$ bond lengths. The relative shortness of Co–$N_{eq}$ bond lengths vis a vis Fe–$N_{eq}$ bond lengths in similar complexes (Table II and ref 34 and 35) and the existence of some strain in the chelate rings suggest that the observed regularities are not simply dictated by the stereochemistry of the macrocyclic ligands.

Axial bond lengths in the cobalt(III) complexes vary with the nature of the axial ligand but are independent of the equatorial $N_4$ ligand in the series of complexes investigated. In striking contrast is the dramatic dependence of axial bond lengths on the equatorial ligand for the cobalt(II) complexes. It appears that the axial $Co^{II}$–$OH_2$ bond is very susceptible to distortions induced by nonbonded repulsive (steric) or electronic interactions with substituents of the equatorial ligand. These structural variations do map out the spatial distribution of the single unpaired and antibonding electron of the $Co^{II}(N_4)(OH_2)_2$ complexes; this electron density lies along the axial (*z*) coordinate and can be conveniently ascribed to a "$d_{z^2}$" orbital.[21c]

That the coordination sphere bond lengths of $Fe(Me_4[14]tetraeneN_4)(OH_2)_2^{3+}$ are not all longer than those of the isomorphous $Co(Me_4[14]tetraeneN_4)(OH_2)_2^{3+}$ is surprising. This may indicate a small coordination sphere distortion of the low-spin $d^5$ complex.

**B. $Co(N_4)(OH_2)_2^{3+,2+}$ Self-Exchange Rates.** Self-exchange rate constants for the $Co(N_4)(OH_2)_2^{3+,2+}$ reactions have been extracted from the $Co(N_4)(OH_2)_2^{3+}/Co(N_4')(OH_2)_2^{2+}$ cross reaction data in Table III by using $\Delta G_{ab}^* = {}^1/_2(\Delta G_{aa}^* + \Delta G_{bb}^*) + 0.5\Delta G_{ab}^\circ$. For most of the reactions, the free-energy term is very small or zero. Consequently, our approach is nearly equivalent, treating the cross-reaction rate constant as the geometric mean of the self-exchange reaction rate constants for a homologous series of reactants.[36] We have averaged the self-exchange rates thus obtained over all the combinations of reactants examined. The resulting self-exchange parameters are presented in Table IV. This analysis assumes that the work terms are equal for all the reactions examined. Figure 2 demonstrates that this analysis gives a self-consistent set of parameters. These parameters together with[4]

$$\Delta G_{ab}^* = {}^1\!/_2(\Delta G_{aa}^* + \Delta G_{bb}^*) + {}^1\!/_2\Delta G_{ab}^\circ + \frac{(\Delta G_{ab})^2}{8(\Delta G_{aa}^* + \Delta G_{bb}^*) - 8w_{ab}} \quad (7)$$

may be used to predict the rates of the $Ru(NH_3)_6^{2+}$ and $Co(sep)^{2+}$ reductions of $Co(N_4)(OH_2)_2^{3+}$ (Figure 2). Self-exchange parameters in Table IV constitute in part a correction of the earlier, preliminary report.[20e,36-38]

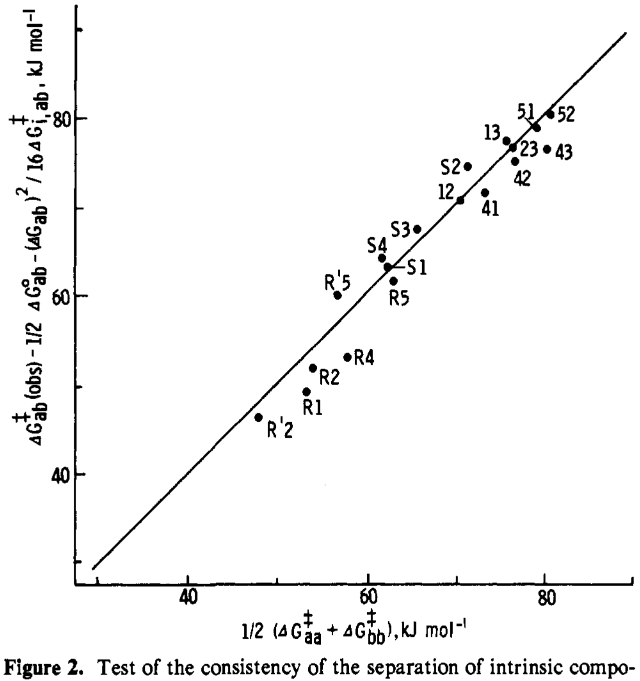

**Figure 2.** Test of the consistency of the separation of intrinsic components for reactions of macrocyclic complexes. Intrinsic reorganizational parameters, $\Delta G_{ij}^*$, have been separated as described in the text (see Table V). For several cross reactions the mean values of reactant intrinsic parameters (abscissa) are compared to the overall intrinsic parameters estimated by using eq 7 (ordinate). The solid line is drawn with unitary slope to pass through the origin. Integers and letters indicate the reactant partners (reductant, oxidant): 1, $Co(Me_2pyo[14]trieneN_4)(OH_2)_2$; 2, $Co(Me_4[14]tetraeneN_4)(OH_2)_2$; 3, $Co(Me_2[14]1,11\text{-}dieneN_4\text{-}13\text{-}one)(OH_2)_2$; 4, $Co([14]aneN_4)(OH_2)_2$; 5, $Co(Me_6[14]4,11\text{-}dieneN_4)(OH_2)_2$; S, $Co(sep)^{2+}$; R, $Ru(NH_3)_6^{2+}$; R′, $Ru(NH_3)_5py^{2+}$. All data referenced to $\mu = 1$, 25 °C. Reaction R2 is from ref 20b, R5, from ref 20a, and the remainder from this study.

**C. Structure-Reactivity Correlations in Reactions of $Co(N_4)(OH_2)_2^{3+,2+}$ Couples: The First Coordination Sphere Reorganizational Energy.** Self-exchange rates for the $Co(Me_4[14]tetraeneN_4)(OH_2)_2^{3+,2+}$, $Co(Me_2[14]1,11\text{-}dieneN_4\text{-}13\text{-}$

---

(34) (a) Smith, H. W.; Santarsiero, B. D.; Lingafelter, E. C. *Cryst. Struct. Commun.* **1979**, *8*, 49. (b) Torre, L. P. Ph.D. Dissertation, University of Washington, 1978. (c) Lingafelter, E. C., private communication, 1979.

(35) We are grateful to Professor E. L. Lingafelter for providing information concerning these structure determinations in advance of publication.

(36) The low-spin $Co(N_4)(OH_2)_2^{3+,2+}$ couples are very closely related in molecular and electronic structure. As a consequence, we believe that the procedure described provides an accurate collection of self-exchange parameters. However, some caution is appropriate as we have inferred below that these reactions are significantly "nonadiabatic". The correlation in Figure 4 suggests that the two-center electron-exchange integral (or, in a semiclassical formulation, the electronic transmission factor) is nearly constant through this series of compounds. However, such constancy need not obtain, as has been strikingly illustrated by the observation that the $Co(sep)^{2+}/Co(en)_3^{3+}$ reaction (for which $K_1 \approx 3$) has a rate constant of ~7 $M^{-1}\ s^{-1}$ at 25 °C, $\mu = 0.5$ (Kumar, K.; Endicott, J. F., work in progress); this is about $10^2$ larger than the prediction based on eq 7. This discrepancy may be related to the densities of electronic states in the high-spin cobalt(II)–low-spin cobalt (III) couples and their effect on the electron-exchange integral. This matter is being investigated further.

(37) An ion-exchange procedure had to be used for separation of cobalt-60 labeled $Co(Me_6[14]4,11\text{-}dieneN_4)(OH_2)_2^{3+}$ and $Co(Me_6[14]4,11\text{-}dieneN_4)(OH_2)_2^{2+}$ species. Nearly all the attempts were complicated by separation-induced exchange or oxidation of the cobalt(II) complex; the cobalt(II) complex had not been characterized at the time (1968–1969) this early study was initiated. Our studies of the $Co(d_{12}Me_4[14]tetraeneN_4)(OH_2)_2^{3+}/Co(Me_4[14]tetraeneN_4)(OH_2)_2^{2+}$ exchange[20e] was complicated by a then unsuspected base-induced reaction of the macrocyclic ligand during the attempted deuterations; i.e., treatment of $Co(Me_4[14]tetraeneN_4)(OH_2)_2^{3+}$ with base initially results information of a new $Co^{II}(N_4)$ complex, and the cobalt(III) species obtained on acidification appears to have additional unsaturation in the equatorial ligand.[38]

(38) (a) Endicott, J. F.; Durham, B. In "Coordination Chemistry of Macrocyclic Compounds"; Melson, G. A., Ed.; Plenum Press: New York, 1979; Chapter 6, p 393. (b) Durham, B. Ph.D. Dissertation, Wayne State University, 1977.

(39) Several attempts using laser Raman techniques and aqueous solutions of $Co(N_4)(OH_2)_2$ complexes have failed to find peaks in the 500–200-cm$^{-1}$ region which are sensitive to deuteration. Apparently the Co–$OH_2$ frequencies are broad and weak. Hydrogen-bonded coupling of coordinated and solvent water may be a major complicating feature. The force constants we have used assume the trans-interaction terms are negligible; i.e., for $f_i = f_{ML} + f_{L\text{-}M\text{-}L}$, we have assumed $f_{L\text{-}M\text{-}L} \ll f_{ML}$. This assumption is probably reasonable for Co(III), but not for Co(II), and we probably underestimate the Franck-Condon factor in Figure 4.

Table VI. $Ru(NH_3)_6^{2+}$ and $Co(sep)^{2+}$ Reductions of $Co(N_4)(OH_2)_2^{3+}$ Complexes (Medium = 0.1 M $HClO_4$

| $N_4$ | $10^4[Co^{III}N_4]$, M | $10^4$[reductant],[a] M | $10^{-4}k$,[b] $M^{-1}\ s^{-1}$ | $10^{-5}k$ ($\mu$ = 1),[c] $M^{-1}\ s^{-1}$ |
|---|---|---|---|---|
| A. $Ru(NH_3)_6^{2+}$ Reactions | | | | |
| $Me_2pyo[14]trieneN_4$ | 1.0–23 | 1.8–32 (10) | (4.75 ± 0.06) | 7.8 |
| $Me_2[14]1,11\text{-}dieneN_4\text{-}13\text{-}one$ | 1.5–13 | 1.8–12.4 (6) | 12.0 ± 0.10 | 19 |
| B. $Co(sep)^{2+}$ Reactions | | | | |
| $Me_2pyo[14]trieneN_4$ | 10–21 | 2.96 (3) | 5.4 ± 0.2 | 7.8 |
| $Me_4[14]tetraeneN_4$ | 8–16 | 1.41 (5) | 6.8 ± 0.2 | 11 |
| $Me_2[14]1,11\text{-}dieneN_4\text{-}13\text{-}one$ | 2.7 | 10–14 (2) | 3.0 ± 0.2 | 4.46 |
| $Me_6[14]4,11\text{-}dieneN_4\text{-}one$ | 1.4 | 10–21 (3) | 0.079 ± 0.003 | 0.124 |
| $[14]aneN_4$ | 25.6 | 2.8 (2) | (6.5 ± 0.1) × $10^{-3}$ | 0.010 |

[a] Number of determinations in parentheses. [b] 25 °C. [c] Extrapolation based on the ionic strength dependence of the $Ru(NH_3)_6^{2+}/Co(NH_3)_5Br^{2+}$ reaction.

one)$(OH_2)_2^{3+,2+}$, and $Co(Me_6[14]4,11\text{-}dieneN_4)(OH_2)_2^{3+,2+}$ couples become smaller as the apparent bond length change (axial $Co^{III}$–$OH_2$ to axial $Co^{II}$–$OH_2$) becomes larger. In fact if we consider also the $Ru(bpy)_2(NH_3)_2^{3+,2+}$ couple for which the bond length change $\Delta X$ (in pm) is negligible, for which the external dimensions average about the same as those of the macrocyclic complexes and for which $k_{exch} \simeq 4 \times 10^8\ M^{-1}\ s^{-1}$ ($\mu$ = 1.0, 25 °C),[11] then excellent empirical correlation for these four systems is (in kJ $mol^{-1}$) $\Delta G_{exch}^{*} = (8.4 \pm 0.3) + (0.73 \pm 0.06)\Delta X$. The intercept term ($\Delta X = 0$) is a measure of the contributions of work terms and solvent reorganizational energies for these systems at ionic strength of 1.0.

One may use either a classical (harmonic oscillator) or quantum model to evaluate the reorganizational energy associated with changes in metal–ligand bond length. In the classical limit

$$\Delta G_r^{*} = \frac{n}{2}\,\frac{f_{II}f_{III}}{f_{II} + f_{III}}\,\Delta X^2 \tag{8}$$

where $n$ is the number of bonds and $f_{II}$ and $f_{III}$ are the corresponding force constants[39] for the divalent and trivalent metals, respectively. Unfortunately we have been unable to determine the symmetrical stretching frequencies of the axial ligands in $Co(N_4)(OH_2)_2$ complexes.[40] In principle, $f_{ML} = \partial^2U/\partial r^2$ where $U$ is the potential energy of the metal–ligand interaction and $r$ is the metal–ligand distance.[40] This would suggest a correlation of $f_{ML}$ with $(Z/r_{ML}^3)$ since heats of hydration are correlated with $1/r_{ML}$[41] (this is actually a variation of Badger's rule[42]). The resulting empirical correlation between $f_i$ and $Z/r_{ML}^3$ is very good for the $a_{1g}$ mode of hexaammine[43] and hexaaquo complexes of the first-row transition elements (Table S6, Figure 3). We have used this correlation to estimate force constants (and vibrational frequencies) of the symmetrical stretching modes of $Co(N_4)(OH_2)_2$ complexes and of the breathing modes of Co(sep) complexes (Table V).

The dominant term in the Franck–Condon factor of the quantum model developed by Buhks et al.[19] is effectively the quantum equivalent of (8) and may be expressed (for $\Delta G° = 0$)[44]

$$\Delta G_r^{*}/RT = \frac{2\omega_{II}\omega_{III}nM(\Delta X^2/\hbar)}{\omega_{II}\coth\nu_{III} + \omega_{III}\coth\nu_{II}} \tag{9}$$

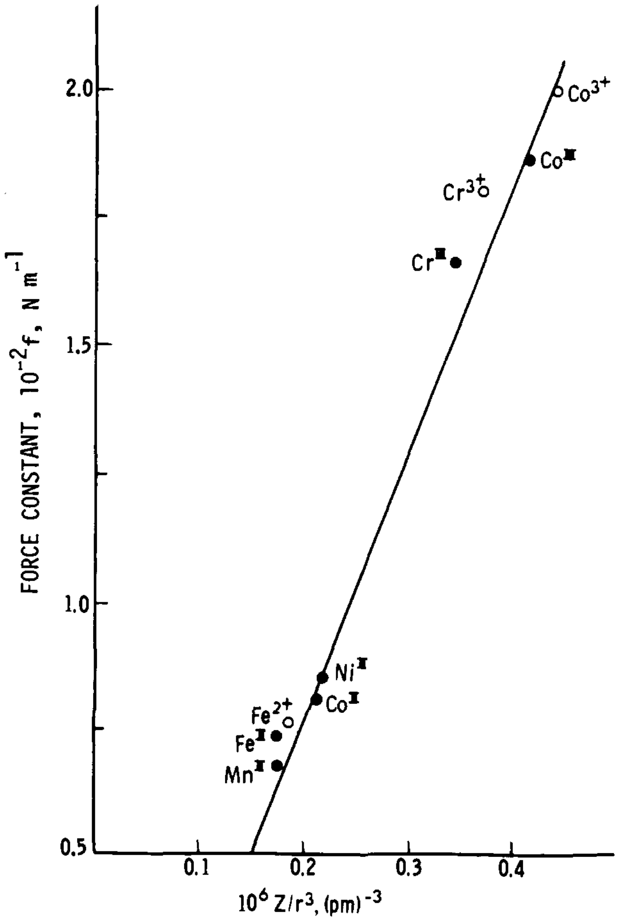

**Figure 3.** Correlation with bond length of the force constants of the $a_{1g}$ modes of several $ML_6$ complexes. Force constant data from ref 42 and Nakamoto, K. "Infrared Spectra of Inorganic and Coordination Compounds", 2nd ed.; Wiley Interscience: New York, 1970. Bond lengths are from X-ray structural data (tabulated in ref 42 and elsewhere; see Table SVI): open circles, $M(OH_2)_6^{n+}$; closed circles, $M(NH_3)_6^{n+}$.

where $\omega_{II}$ and $\omega_{III}$ are the critical metal–ligand vibrational frequencies (subscripts indicating the formal oxidation states), $n$ is the number of bonds involved in the critical metal–ligand motion, $M$ is the reduced mass, and $\nu_i = \hbar\omega_i/4k_BT$. Equation 9 results in a slightly smaller value for $\Delta G_r^{*}$ than does the use of eq 8; see Figure 4 and ref 11 and 44; if differences in preexponential terms were taken into account, the classical and quantum mechanical Franck–Condon factors would be even more similar. This very small difference in Franck–Condon factors estimated by classical and quantum approaches is a necessary consequence of the small values of the metal–ligand vibrational frequencies, especially $\omega_{II}$, since $\hbar\omega_i < 4kT$ at room temperature.

The differences in self-exchange electron-transfer rates are in excellent agreement with the expected variations in contributions of the Franck–Condon factors for the cobalt(III)–cobalt(II)

---

(40) Basolo, F.; Pearson, R. G. "Mechanisms of Inorganic Reactions"; Wiley: New York, 1967.

(41) Philips, C. S. G.; Williams, R. J. P. "Inorganic Chemistry"; Clarendon Press: Oxford, 1965; pp 161–162.

(42) Badger, R. M. *J. Chem. Phys.* **1934**, *2*, 128; **1935**, *3*, 710.

(43) (a) Schmidt, K. H.; Muller, A. *Inorg. Chem.* **1975**, *14*, 2183. (b) Cyrin, B. N.; Cyrin, S. J.; Schmidt, K. H.; Muller, A. *Coord. Chem. Rev.* **1976**, *21*, 221.

(44) Equation 9 is the dominant exponential component of the average Franck–Condon terms for a system with a single contributing, quantized vibrational mode. There will also be some variation of the preexponential terms with $(\Delta X)^2$. We estimate these other terms to contribute only 1–3 kJ $mol^{-1}$ to the apparent value of $\Delta G_i^{*}$. It should also be noted that (9) reduces (8) for $h\omega_i << 4k_BT$. Further, $\Delta G_r^{*}(Q)/RT$ calculated from (9) must always be smaller than $\Delta G_r^{*}(C)/RT$ calculated from (8) (e.g., see ref 11). In the limit, $\Delta G_r^{*}(C)/\Delta G_r^{*}(Q) \approx \hbar\omega/4kT >> 1$.

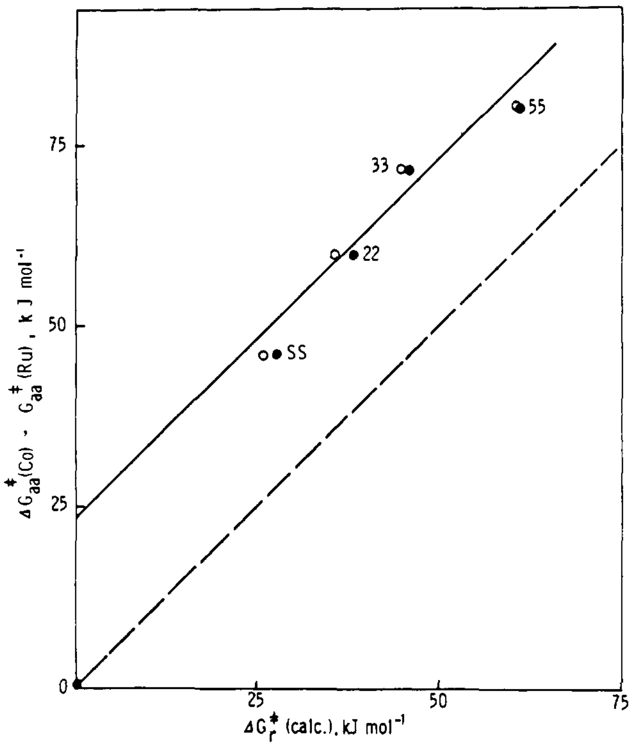

**Figure 4.** Comparison of the intrinsic barrier to electron transfer, $\Delta G_{aa}^*$, with the calculated reorganizational energies: (a) solid circles, harmonic oscillator approximation, eq 8; (b) open circles, allowing for vibrational quantization using eq 9. Numbering convention for cobalt couples as in Figure 2. Each value of $\Delta G_{Co}^*$ has been decreased by $\Delta G_{Ru}^*$, for the $Ru(bpy)_2(NH_3)_2^{3+,2+}$ self-exchange;[12] this has been chosen as a reference couple because the external dimensions are similar to those of $Co(N_4)(OH_2)_2$ complexes and $\Delta X \sim 0$. Force constants have been estimated from a $f_i \simeq z/r^3$ correlation of the $a_{1g}$ vibrations of $ML_6$ complexes (see Figure 3). The dashed line has been drawn through the origin and has unitary slope. The solid line correlates the cobalt self-exchange data and also has unitary slope.

couples (i.e., eq 8 or 9). However, the intercept ($\Delta G_{Co}^*$ ($\Delta X = 0$)) of the correlation of $\Delta G_{Co}^*$ with $\Delta G_r^*$ is about 20 kJ mol$^{-1}$ greater than the value of $\Delta G^*$ reported for the $Ru(bpy)_2(NH_3)_2^{3+,2+}$ couple. The mean diameter of this ruthenium complex is very similar to that of the cobalt macrocycle complexes. Since the $Ru^{II}$–N and $Ru^{III}$–N bond lengths are undoubtedly very similar,[12,18] the self-exchange rate constant of the ruthenium couple can be taken as an experimental measure of the contribution of Coulombic work terms and solvent reorganizational terms for 3+/2+ couples of this size. A small part of the discrepancy between $\Delta G_{Ru}^*$ and $\Delta G_{Co}^*$ ($\Delta X \rightarrow 0$) could result from different specific interactions of cobalt and ruthenium complexes with counterions or with solvent molecules. Since the $Co(sep)^{3+,2+}$ couple correlates very well with the cobalt–macrocycle complexes, it seems unlikely that specific interactions between reactant and medium species can vary a great deal among the reactants considered. The approximations we have used in estimating force constants[39] undoubtedly result in an underestimate of Franck–Condon factors. As a consequence, the actual discrepancy of the intercept in the comparison represented in Figure 4 is probably only about 10 kJ mol$^{-1}$.

The quantum mechanical formulation of the electron-transfer rate constant may be expressed $k = N_0 f(\bar{R}) W$, where $f(\bar{R})$ depends only on external distance parameters and should be very similar for the cobalt and ruthenium complexes, $N_0$ in concentration unit and $W$ in a transition probability. The two important factors of $W$ are the two-center electron-exchange integral $V_{if}$ and the Franck–Condon term.[19] Both factors contribute to the rate differences between $Co(NH_3)_6^{3+,2+}$ and $Ru(NH_3)_6^{3+,2+}$,[19] and both factors may contribute to the rate difference we find between the $Co(N_4)(OH_2)_2^{3+,2+}$ and $Ru(bpy)_2(NH_3)_2^{3+,2+}$ couples. The semiclassical formulation is approximately equivalent to the quantum formulation and represents the rate constant as[11]

$$k = \kappa_{el}\Gamma Z e^{-\Delta G^*(C)/RT}$$

where $\kappa_{el}$ is the electronic transmission coefficient, $\Gamma$ is a tunneling factor, $Z$ is the classical preexponential term, and $\Delta G^*(C)$ is the classical reorganizational barrier. Since the classical and quantum evaluations of the Franck–Condon barrier give such similar results, $\Gamma$ must be nearly unitary. Our analysis would place $\kappa_{el}$ in the range of $10^{-2}$–$10^{-4}$ for the cobalt complexes. One would expect $V_{if}$ (and therefore $\kappa_{el}$) to be smaller in cobalt(III)–cobalt(II) couples ($\sigma_M^*$–$\sigma_M^*$ electron-exchange systems) than in ruthenium(III)–ruthenium(II) couples ($\pi_M$–$\pi_M$ electron-exchange systems). The value of $V_{if}$ should be even smaller for low-spin cobalt(III)–high-spin cobalt(II) couples[19] such as $Co(sep)^{3+,2+}$. However, we find no evidence for an additional effect.

**D. Free-Energy Dependence of Cross Reactions Involving $Co(N_4)(OH_2)_2^{3+,2+}$ Couples.** Our early studies of these systems suggested some discrepancies between the form of eq 7 and the observed free-energy dependencies of cross reactions involving $Co(N_4)(OH_2)_2^{3+,2+}$ couples.[21] To some degree these inferences were flawed by the inaccuracy of the preliminary estimates of self-exchange rate constants for the $Co(Me_4[14]tetraeneN_4)(OH_2)_2^{3+,2+}$ and $Co(Me_6[14]4,11\text{-}dieneN_4)(OH_2)_2^{3+,2+}$ couples[20e,37] and by the usual lack of crucial thermodynamic and self-exchange parameters for reactions involving labile cobalt(II) partners[10b] (e.g., ammine, amine, oxalate, etc. complexes). Nevertheless, the quantum mechanical treatments of electron-transfer reactions[7,8,19] suggest that the variation of $\Delta G_{ab}^*$ with $\Delta G_{ab}^\circ$ may be very complex for reactions involving large changes in bond lengths in the first coordination sphere. The more accurate information, which has become available during the past 5 years regarding reactions of these complexes with several partners, permits a more critical examination of this question.

In order to facilitate the present discussion, it is useful to put eq 7 in the form

$$\frac{\Delta G_{ab}^* - w}{\Delta G_{i,ab}^* - w} = \left(1 + \frac{\Delta G_{ab}^\circ}{4(\Delta G_{i,ab}^* - w)}\right)^2 \qquad (10)$$

where the intrinsic barrier, $\Delta G_{i,ab}^* = {}^1/_2[\Delta G_{aa}^* + \Delta G_{bb}^*]$, and the work terms of 3+/2+ couples are all assumed to be equal at $\mu = 1$ (we have set $w = 6.7$ kJ mol$^{-1}$ in the figures and in Table SV.[33] Equations 7 and 10 represent a specific case of a more general relationship[46,47]

$$\frac{\Delta G_{ab}^* - w}{\Delta G_{i,ab} - w} = \alpha\frac{\Delta G_{ab}^\circ}{\Delta G_{i,ab} - w} + M(\alpha) \qquad (11)$$

where $\alpha$ is the Brønsted coefficient and $M(\alpha)$ is a function of $\alpha$. It is convenient to rewrite eq 11 as

$$F(y) = \alpha y + M(\alpha) \qquad (12)$$

where $F(y) = (\Delta G_{ab}^* - w)/(\Delta G_{i,ab}^* - w)$ and $y = G_{ab}^\circ/(\Delta G_{i,ab}^* - w)$. For a physically meaningful representation of kinetic data to be provided, eq 12 must have the properties: (1) $F(y = 0) = 1.0$ and (2) $F(y) = F(-y) + y$ (since $K_{ab} = k_{ab}/k_{ba}$). Most of the experimental data available from studies in the region $-\Delta G_{ab}^\circ > 4(\Delta G_{i,ab}^* - w)$ indicates[48,51] that as $y \rightarrow -\infty$, $F(y) \rightarrow 0$. This leads to the empirical condition: (3) $\lim_{y\rightarrow-\infty} F(y) = 0$. Several functional relationships of $\Delta G_{ab}^*$, $\Delta G_{ab}^\circ$ and $\Delta G_{i,ab}^*$ have been proposed:

---

(45) Wilson, R. B.; Solomon, E. I. *J. Am. Chem. Soc.* **1980**, *102*, 4085.

(46) Marcus, R. A. *J. Phys. Chem.* **1968**, *72*, 891.

(47) Levine, R. D. *J. Phys. Chem.* **1979**, *83*, 159.

(48) Brunschwig, B.; Sutin, N. *J. Am. Chem. Soc.* **1978**, *100*, 7568.

(49) Scandola, F.; Balzani, V. *J. Am. Chem. Soc.* **1979**, *101*, 6140.

(50) Nagle, J. K.; Dressick, W. J.; Meyer, T. J. *J. Am. Chem. Soc.* **1979**, *101*, 3993.

(51) (a) Rehm, D.; Weller, A. *Isr. J. Chem.* **1970**, *8*, 259. (b) *Ber. Bunsenges.* Phys. *Chem.* **1969**, *73*, 834.

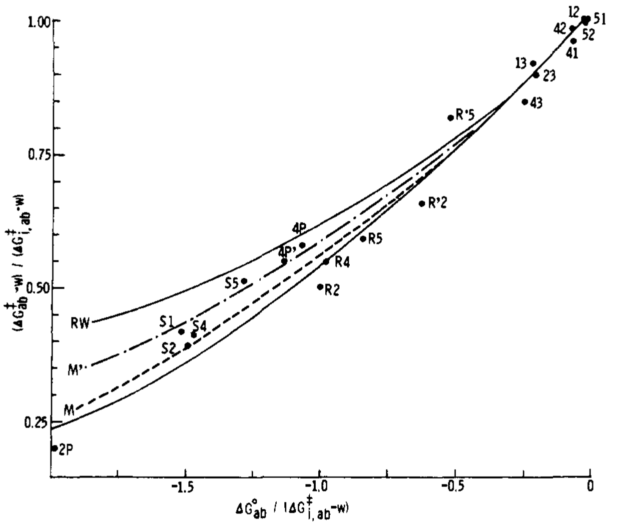

**Figure 5.** Examination of the free-energy, $G_{ab}^{\circ}$, dependence of outer-sphere electron-transfer reactions of $Co(N_4)(OH_2)_2$ complexes. Conventions are as in Figure 4, except the following: 2P, $Co(Me_4[14]tetraeneN_4)(OH_2)_2^{2+}$ + $Ru(bpy)_3^{3+}$; 4P, $Co([14]aneN_4)(OH_2)_2^{2+}$ + $Fe(bpy)_3^{3+}$; 4P′, $Co([14]aneN_4)(OH_2)_2^{2+}$ + $Fe(phen)_3^{3+}$. (The $Fe(PP)_3^{3+}$ reactions are from: Wong, C.-L.; Endicott, J. F. submitted for publication in *Inorg. Chem.*) The solid line is drawn to have relatively little curvature. The dashed and dotted lines correspond to the various algebraic relationships discussed in the text: M, eq 13; M′, eq 14; R and W, eq 15.

(1) Marcus proposed[4] that for weak donor–acceptor interactions and in a "semi classical" limit, electron-transfer reactions should be described by

$$F(y) = 1 + y/2 + y^2/16 \qquad (13)$$

(2) For group-transfer reactions Marcus[46] proposed

$$F(y) = 1 + y/2 + \frac{1}{\ln 2}\ln[\cosh(\tfrac{1}{2}y \ln 2)] \qquad (14)$$

It is to be noted that (14) reduces to (13) only for $|\Delta G^{\circ}| << 4(\Delta G_{i,ab} - w)$.

(3) Rehm and Weller[51] proposed an empirical equation to describe electron-transfer reactions

$$F(y) = y/2 + [y^2/4 + 1]^{1/2} \qquad (15)$$

Of these equations, only (14) and (15) are in accord with the empirical condition 3, noted above.

In order to examine the dependence of $\Delta G_{ab}^{\ddagger}$ on $\Delta G_{ab}^{\circ}$, we have examined the $Co(sep)^{2+}/Co(N_4)(OH_2)_2^{3+}$ reactions and we have extended the earlier work[21a] on $Ru(NH_3)_6^{2+}/Co(N_4)(OH_2)_2^{3+}$ reactions. Earlier studies of $M(pp)_3^{3+}$ (pp = polypyridyl) oxidations of $Co(N_4)(OH_2)_2^{2+}$ complexes were performed in a sulfuric acid medium[20d] and cannot be directly compared with the present data obtained in perchloric acid media. Over a limited range of the free energy parameter ($0 \le y \le 2$) accumulated errors in the ratios of experimental quantities result in appreciable scatter in a plot of F($y$) vs. $y$ (Figure 5). Nevertheless, it is evident that (13) and (14) provide better descriptions of the results over this range than does (15).

It is extremely difficult to investigate the variations of $F(y) = (\Delta G_{ab}^{\ddagger} - w)/(\Delta G_{i,ab}^{\ddagger} - w)$ with $y$ over an extended range of $y$ for redox couples involving large changes in metal–ligand bond length ($\Delta X$ large) since this results in large values of $\Delta G_{i,ab}^{\ddagger}$. For our complexes, such investigations would require $\Delta G_{ab}^{\circ} \gtrsim 250$ kJ mol$^{-1}$. Thus in an investigation of the extended range of the variation of $\Delta G_{ab}^{\ddagger}$ with $\Delta G_{ab}^{\circ}$, one must generally resort to complexes with small intrinsic barriers ($\Delta G_{i,jj}^{\ddagger} \le 12$ kJ mol$^{-1}$). Data for one such reaction is included in Figure 6. It is clear that (14) gives a reasonable overall fit to the data considered. However, we must emphasize that values of $(\Delta G_{ab}^{\ddagger} - w)/(\Delta G_{i,ab}^{\ddagger} - w)$ become very sensitive to the quality of the estimates of $\Delta G_{i,ab}^{\ddagger}$ and $w$ as ($-y$) becomes very large; thus for the $Ru(bpy)_3^{3+}/Cr(bpy)_3^{2+}$ reaction we would estimate that $F(y) \approx 0.8 \pm 0.7$. This is equivalent to an uncertainty in the width of the parabolic curve predicted by the familiar Marcus relation (7) and is an issue raised previously by Brunschwig and Sutin.[48] Owing to the manner in which $\Delta G_{ab}^{\circ}$ and $\Delta G_{i,ab}^{\ddagger}$ appear to be coupled (e.g., (13), (14), and (15)), the uncertainty in the free-energy dependence of $\Delta G_{ab}^{\ddagger}$ when $(\Delta G_{ab}^{\circ}) >> 4(\Delta G_{i,ab}^{\ddagger} - w)$ is unavoidable. In this regard plots of $\Delta G_{ab}^{\ddagger}$ vs. $\Delta G_{ab}^{\circ}$ can be very misleading. For similar reasons, arbitrary adjustment of work terms can be employed to fit data to any presumed functional dependence[52] of $\Delta G_{ab}^{\ddagger}$ on $\Delta G_{ab}^{\circ}$, but the significance of such manipulations is questionable. On balance it appears that meaningful discrimination among proposed free-energy dependences of electron-transfer reactions in the highly exoergic region can only be made for a series of reactions in which $\Delta G_{i,ab}^{\ddagger}$ and the various work terms are small, but rigorously constant. It may not be experimentally feasible to make such studies sufficiently critical to distinguish among all the models proposed although studies with polypyridyl complexes may approach such conditions.[48-50] Unfortunately the highly exoergic region appears to be inaccessible for complexes with large first coordination sphere reorganization energies. However, Figures 5 and 6 do not indicate any difference in the $\Delta G_{ab}^{\circ}$ dependence of reactions for reactions with $\Delta X$ large from those in which $\Delta X = 0$.

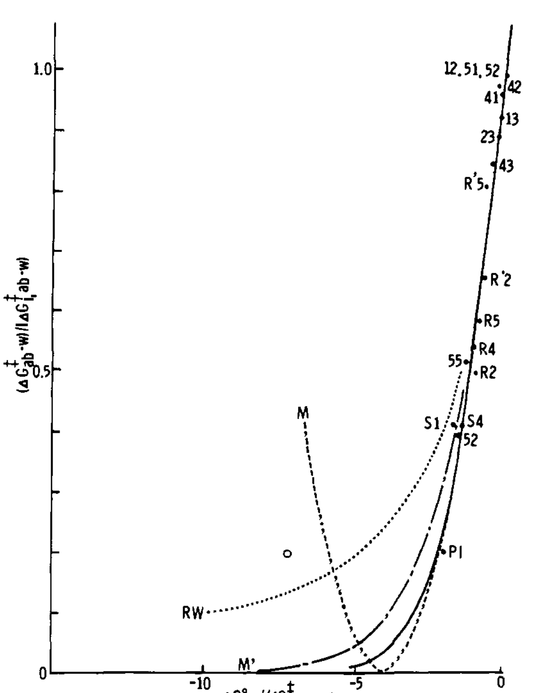

**Figure 6.** Free-energy dependence of outer-sphere electron-transfer reactions considered over an extended range. Curves and data points are as in Figure 4; the open circle is for the $Ru(bpy)_3^{3+}/Ru(NH_3)_6^{2+}$ reaction.

Some general features of the free-energy dependence of electron-transfer reactions warrant additional comment. The solid curve drawn to fit the data points in Figure 5 exhibits slightly less curvature than any of the free-energy functions proposed above. This may be expressed in terms of the Brønsted coefficient, $\alpha = \partial F(y)/\partial y$. The empirical function fitted to these data would give $\alpha$ near to 0.5 over an extended range of $\Delta G_{ab}^{\circ}/(\Delta G_{i,ab}^{\ddagger} - w)$. This is reasonably well approximated by $\alpha = \frac{1}{2}(1 + y/4)$ in the conventional Marcus–Hush treatment.[4,5,46] A physical interpretation of this situation is that for the weakly coupled, outer-sphere electron-transfer reactions the metal centers are separately activated and in the transition state there is nearly equal probability of occupation of donor and acceptor orbitals ($\alpha$ may be interpreted as the transfer coefficient). This is in contrast to group-transfer

---

(52) Weaver, M. J.; Yee, E. L. *Inorg. Chem.* **1980**, *19*, 1936.

reactions in which the stronger coupling between reactant centers can lead to a stronger dependence on the donor–acceptor energy gap.

In the extreme free-energy region ($-\Delta G_{ab}^{\circ} > 4[\Delta G_{i,ab}^{*} - w]$), most available evidence suggests that $\alpha$ approaches zero. However, quantum mechanical models,[7,8a] in which the relaxation from reactant pair to product pair is treated as an isoenergetic tunneling process, predict some variation of $\alpha$ in this region. In most of the systems investigated to date for which $|\Delta G_{ab}^{\circ}| > 4(\Delta G_{i,ab}^{*} - w)$, $\Delta X \approx 0$, and the potential energy surfaces of reactant and product pairs are distinguishable only owing to the nearly classical motions of the surrounding solvent molecules. It seems unlikely that the resulting reactant and product potential energy surfaces would be sufficiently well-defined that quantum constraints on the transition are meaningful. In this regard, investigation of the highly exoergic region of systems in which $\Delta X$ is reasonably large would be very useful.

## Conclusions

The axial bond lengths in low-spin $Co(N_4)(OH_2)_2^{2+}$ complexes are tens of picometer longer than the $Co-OH_2$ bond lengths in cobalt(III) complexes. Rate variations of outer-sphere (self-exchange) electron-transfer reactions of the $Co(N_4)(OH_2)_2^{3+,2+}$ couples are largely dictated by the resulting differences in first coordination sphere reorganizational barriers. These rate variations are in accord with either quantum or classical mechanical descriptions of the Franck–Condon barrier. Comparisons with the self-exchange rate of the $Ru(bpy)_2(NH_3)_2^{3+,2+}$ couple suggest that the $Co(N_4)(OH_2)_2^{3+,2+}$ self-exchange reactions are "nonadiabatic" with $\kappa_{el} \approx 10^{-3\pm1}$. The free-energy dependence of the reaction rates for oxidations of $Co(N_4)(OH_2)_2^{2+}$ and reductions of $Co(N_4)(OH_2)_2^{3+}$ complexes is adequately described by the classical expressions obtained by Marcus.

**Acknowledgment.** The authors are grateful to Drs. R. Sriram and G. J. Ferraudi for assistance with some of the experiments. The authors are very grateful to Professor M. J. Weaver for his careful electrochemical studies of the macrocyclic complexes, and for communicating his results in advance of publication.

**Supplementary Material Available:** Tables of atomic parameters, of kinetic parameters, and of force constants and bond lengths (18 pages). Ordering information is given on any current masthead page.

---

# How Niobium and Tantalum Complexes of the Type $M(CHCMe_3)(PR_3)_2Cl_3$ Can Be Modified To Give Olefin Metathesis Catalysts[1]

**S. M. Rocklage, J. D. Fellmann, G. A. Rupprecht, L. W. Messerle, and R. R. Schrock***

*Contribution from the Department of Chemistry, Massachusetts Institute of Technology, Cambridge, Massachusetts 02139.* *Received July 14, 1980*

**Abstract:** Complexes of the type $M(CHR)L_2X_3$ (M = Nb or Ta, R = $CMe_3$ or Ph, L = a tertiary phosphine, X = Cl or Br) react with terminal olefins to give the organic products of $\beta$-hydride rearrangement of the four possible intermediate metallacyclobutane complexes. We see no metathesis products or cyclopropanes. When L = THF or py, the complex reacts with ethylene to give ~10% metathesis product, with 1-butene to give ~50% metathesis products, and with *cis*-2-pentene to give exclusively metathesis products. $Ta(CHCMe_3)(THF)_2Cl_3$ is a short-lived metathesis catalyst for *cis*-2-pentene. Complexes of the type $M(CHCMe_3)(OCMe_3)_2Cl(PMe_3)$ react with terminal and internal olefins to give only metathesis products and are longer lived (ca. 35 turnovers) metathesis catalysts for *cis*-2-pentene. The major chain termination steps in metathesis of a terminal olefin are decomposition (probably intermolecular) of intermediate methylene complexes and rearrangement of intermediate metallacyclobutane complexes. The major chain termination step in metathesis of *cis*-2-pentene is rearrangement of an alkylidene ligand in an intermediate alkylidene complex to an olefin.

## Introduction

The reaction between an alkylidene complex and an olefin is the favorite proposed mechanism for scrambling alkylidene fragments in the olefin metathesis reaction.[2] Therefore we have been interested for some time in how niobium- and tantalum-alkylidene complexes[3] react with olefins. The first type which contained no other potentially reactive ligands which might complicate such studies was $Ta(\eta^5-C_5H_5)(CHCMe_3)Cl_2$.[4] It reacts with terminal olefins to give a tantallacyclobutane complex which rapidly rearranges to an unobservable olefin complex by migration of a $\beta$-proton to an $\alpha$-carbon atom. Two equivalents of the smaller, more strongly coordinating olefin which is present in excess then displaces this new olefin to give a tantallacyclo-

Scheme I. The Four Products Formed on Reacting a Halo/Alkylidene Complex with a Terminal Olefin (See Table I)

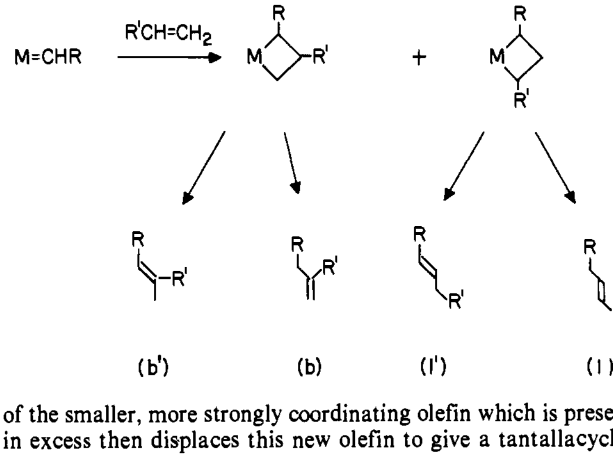

---

[1] Multiple Metal-Carbon Bonds. 19. For part 18 see: Fellmann, J. D.; Turner, H. W.; Schrock, R. R. *J. Am. Chem. Soc.* **1980**, *102*, 6608.

[2] (a) Calderon, N.; Lawrence, J. P.; Ofstead, E. A. *Adv. Organomet. Chem.* **1979**, *17*, 449-492 and references therein. (b) Grubbs, R. H. *Prog. Inorg. Chem.* **1978**, *24*, 1-50.

[3] Schrock, R. R. *Acc. Chem. Res.* **1979**, *12*, 98-104.

[4] Wood, C. D.; McLain, S. J.; Schrock, R. R. *J. Am. Chem. Soc.* **1979**, *101*, 3210-3222.

0002-7863/81/1503-1440$01.25/0